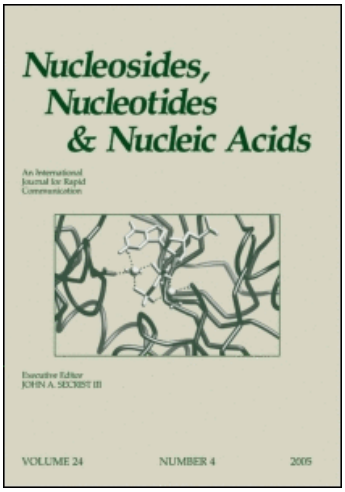

Nucleosides, Nucleotides and Nucleic Acids
Publication details, including instructions for authors and subscription information:
http://www.informaworld.com/smpp/title~content=t713597286

Intercalating Nucleic Acids: The Influence of Linker Length and Intercalator Type on Their Duplex Stabilities

Ulf B. Christensen[ab]; Michael Wamberg[a]; Farag A. G. El-Essawy[a]; Abd El-Hamid Ismail[a]; Christina B. Nielsen[a]; Vyacheslav V. Filichev[a]; Carsten H. Jessen[a]; Michael Petersen[a]; Erik B. Pedersen[a]
[a] Nucleic Acid Center[††], Department of Chemistry, University of Southern Denmark, Odense, Denmark [b] Unest A/S, Odense SØ, Denmark

Online publication date: 02 October 2004

To cite this Article Christensen, Ulf B. , Wamberg, Michael , El-Essawy, Farag A. G. , Ismail, Abd El-Hamid , Nielsen, Christina B. , Filichev, Vyacheslav V. , Jessen, Carsten H. , Petersen, Michael and Pedersen, Erik B.(2004) 'Intercalating Nucleic Acids: The Influence of Linker Length and Intercalator Type on Their Duplex Stabilities ', Nucleosides, Nucleotides and Nucleic Acids, 23: 1, 207 — 225
To link to this Article: DOI: 10.1081/NCN-120027829
URL: http://dx.doi.org/10.1081/NCN-120027829

NUCLEOSIDES, NUCLEOTIDES & NUCLEIC ACIDS
Vol. 23, Nos. 1 & 2, pp. 207–225, 2004

Intercalating Nucleic Acids: The Influence of Linker Length and Intercalator Type on Their Duplex Stabilities†

Ulf B. Christensen,# Michael Wamberg,* Farag A. G. El-Essawy, Abd El-Hamid Ismail, Christina B. Nielsen, Vyacheslav V. Filichev, Carsten H. Jessen, Michael Petersen, and Erik B. Pedersen

Nucleic Acid Center,†† Department of Chemistry,
University of Southern Denmark, Odense, Denmark

ABSTRACT

Six new examples of intercalating nucleic acids were synthesized in order to evaluate the dependence of the length of the linker between oligo and intercalator on the thermal stability of their corresponding duplexes and triplexes.

Key Words: Intercalating nucleic acids; 7,9-Dimethylpyrido[3′,2′:4,5]thieno[3,2-d] pyrimidine-4(1H)-one; Pyrene intercalators; DNA duplex stability of intercalating nucleic acids; Oligonucleotides with covalently bound intercalators.

†In honour and celebration of the 70th birthday of Professor Leroy B. Townsend.

#Current address: Ulf B. Christensen, Unest A/S, Lille Tornbjerg Vej 24 B, DK-5220 Odense SØ, Denmark.

*Correspondence: Michael Wamberg, Department of Chemistry, University of Southern Denmark, Campusvej 55, DK-5230, Odense M, Denmark; Fax: +45-6615-8780; E-mail: mcw@chem.sdu.dk.

††A research center funded by The National Danish Research Foundation for studies on nucleic acid chemical biology.

DOI: 10.1081/NCN-120027829 1525-7770 (Print); 1532-2335 (Online)

INTRODUCTION

Intercalating nucleic acids (INA™s) have recently gained commercial interest for screening DNA methylation signatures in hundreds or thousands of tissue samples when used in combination with the bisulphite DNA conversion technology.[1] The INA™s used for this purpose are synthesized by insertion of 1-*O*-(1-pyrenylmethyl)-glycerol into DNA. This type of INA™s shows a better binding in duplex formation with a very high specificity and is innately fluorescent.[2,3]

We define an intercalating nucleic acid as an oligonucleotide with a covalently bound intercalator. If the intercalator is linked to the backbone one has to consider the structure of the backbone, linker and intercalator in order to evaluate the stability of duplexes when using intercalating nucleic acids for hybridization.

Among others Ossipov et al.[4] are using long linker arms to provide maximum flexibility and to prevent stereochemical alterations of the nucleoside conformation (for hybridizations properties). Also it should be taken into account that the axial distance between two nucleobases are approximately 3.4 Å.[5] Hence it would be optimal if the backbone introduces additionally 3.4 Å between the two neighbouring nucleobases of the strand in which the intercalator is inserted. By introduction of additional flexibility into the backbone of one strand the degree of rotational freedom of this strand is enlarged and hence loss of entropy is larger upon hybridization to a complementary strand. Therefore a minimum degree of flexibility should be introduced, but still enough to support efficient intercalation. In order to fulfil these demands and to make

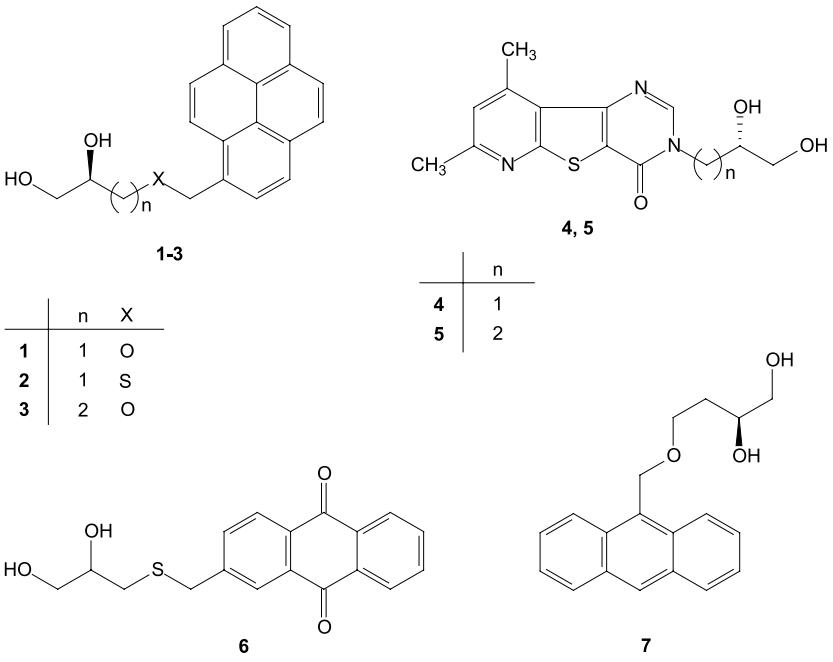

	n	X
1	1	O
2	1	S
3	2	O

	n
4	1
5	2

Figure 1. The seven intercalating nucleic acid monomers used in this investigation.

MARCEL DEKKER, INC.
270 Madison Avenue, New York, New York 10016

an amidite that uses the same chemistry as normal commercial amidites, we chose the vicinal dihydroxy system as the backbone.

If intercalation from an intercalator should increase affinity for the complementary ssDNA, the intercalator has to interact with nucleobases from both the strand in which it is incorporated and the opposite strand. It is therefore the purpose of the linker to place the intercalator in an optimal position for π-interactions with the neighbouring nucleobases, without disrupting the hydrogen bonding of the neighbouring base pairs. The optimal linker length will most likely depend on the size of the intercalator.

The intercalator is the unit that introduces most of the novel features of INA™. It is a compound which contains an essentially flat, conjugated aromatic or heteroaromatic ring system that is able to co-stack with a DNA or RNA duplex. The intercalator is chosen in consideration of several features. The size of the conjugated ring system and the electron density are two influencing factors on the strength of the co-axial stacking. The fluorescence properties of the intercalator are also important for the potential uses of the INA™s.

In order to gain more insight into the above mentioned criteria, seven different intercalating nucleic acid monomers were synthesized (Figure 1) and incorporated into oligonucleotides.

Besides thermal melting studies, we have made structural calculations (Macro-Model) of INA™s and NMR experiments to examine how the intercalator is situated in the duplex.

RESULTS AND DISCUSSION

Chemistry

The synthetic routes towards the intercalating nucleic acid monomers **2–7** are shown in Schemes 1–3, while the monomer **1** has previously been synthesized in our group.[2] **3** and **7** were synthesized starting from chloromethylaryl compounds **8a,b**. The required alcohol (*S*)-2-(2,2-dimethyl-1,3-dioxolane)-4-ethanol was prepared from malic acid as described in the literature,[6,7] and reacted with 1-chloromethylpyrene or 9-chloromethylanthracene in the presence of potassium hydroxide yielding **9a,b**. Subsequent treatment with 80% aqueous acetic acid gave the diols **3** or **7**, which were protected with DMT-chloride to **10a,b** and the products were converted to the phosphoramidites **11a,b** with 2-cyanoethyl *N*,*N*,*N*′,*N*′-tetraisopropylphosphorodiamidite.

The intercalating nucleic acid monomers **4** and **5** were synthesized as shown in Scheme 2. 7,9-Dimethylpyrido[3′,2′:4,5]thieno[3,2-*d*]pyrimidine-4(1*H*)-one **12** was prepared according to literature procedures.[8–10] The tosylates of (*S*)-(+)-2-(2,2-dimethyl-1,3-dioxolane)methanol and (*S*)-(+)-2-(2,2-dimethyl-1,3-dioxolane)-4-ethanol were used for the alkylation reaction to yield **13a,b**. O-alkylation of **12** was also observed. The subsequent three steps towards the phosphoramidites **15a,b** were done as described above for **11a,b**.

For the synthesis of **2** and **6** (Scheme 3) a racemic mixture of 3-mercapto-1,2-propanediol was used in the reaction with 1-chloromethylpyrene **8a** and 2-bromomethylanthraquinone **16b**, respectively. The amidites **18a,b** were obtained by the same protection and phophitylation reactions as in the previous examples, except that

MARCEL DEKKER, INC.
270 Madison Avenue, New York, New York 10016

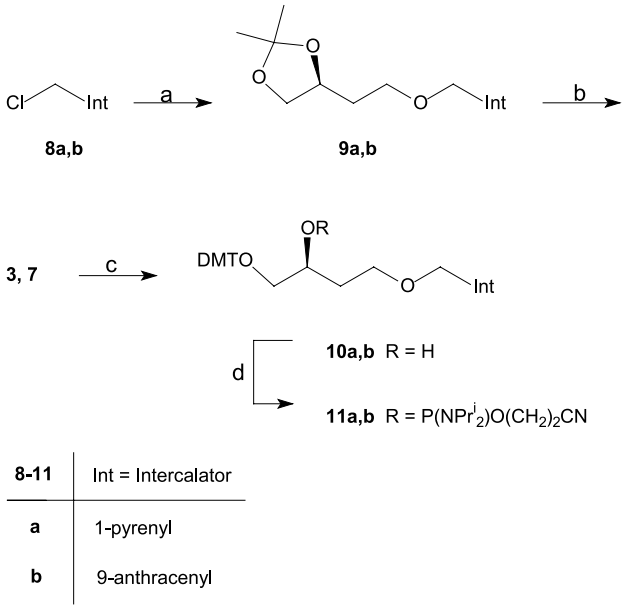

8-11	Int = Intercalator
a	1-pyrenyl
b	9-anthracenyl

Scheme 1. (a) (*S*)-(+)-2,2-dimethyl-1,3-dioxolane-4-ethanol, KOH, toluene, 67–90%; (b) AcOH/H_2O (4:1); (c) DMT–Cl, pyr, 80–85%; (d) NC(CH$_2$)$_2$OP(NPr$^i_2$)$_2$, *N*,*N*-diisopropylammonium tetrazolide, CH_2Cl_2, 62–83%.

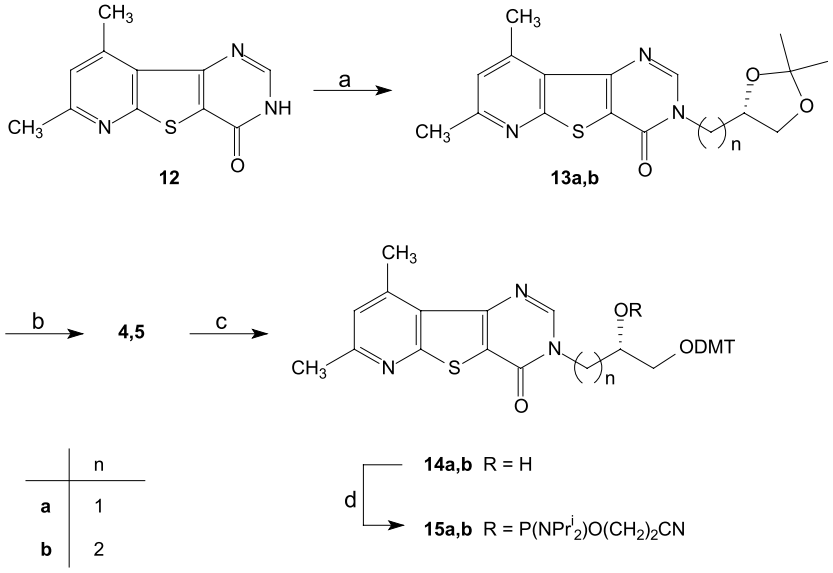

n	
a	1
b	2

Scheme 2. (a) (*S*)-(+)-2,2-dimethyl-1,3-dioxolane-4-ethanoyl-*O*-*para*-toluenesulfonate, NaH, DMF, 45%; (b) AcOH/H_2O (4:1), 75%; (c) DMT–Cl, pyr, 65%; (d) NC(CH$_2$)$_2$OP(NPr$^i_2$)Cl, *N*,*N*-diisopropylammonium tetrazolide, CH_2Cl_2, 84%.

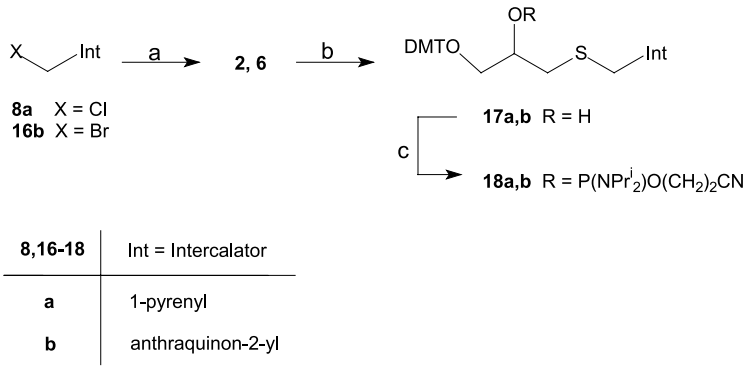

Scheme 3. (a) $HSCH_2CHOHCH_2OH$, toluene or DMF, Et_3N, 78–90%; (b) DMT–Cl, pyr, 66–74%; (c) $NC(CH_2)_2OP(NPr^i_2)Cl$, *N*,*N*-diisopropylammonium tetrazolide, CH_2Cl_2, 62–86%.

2-cyanoethyl *N*,*N*-diisopropylchlorophosphoramidite was used in the last step of the reaction sequence.

The protected phosphoramidites of the intercalating nucleic acid monomers **1–6** were used for insertion of the corresponding monomers into a 12-mer oligonucleotide using the same coupling times (2 min) in the oligo synthesis as was used for the amidites of the natural nucleosides.

Thermal Melting Studies

Except from **3** and **4** all intercalating nucleic acid monomers stabilized the corresponding duplexes when they were inserted as a bulge (Table 1). It is interesting to observe the 6.8°C higher melting temperature for **5** than for **4** when inserted into the duplex. These two compounds differ only in the length of the linker by one atom. The linker seems too short in case of **4** which results in a lower duplex stability. On the contrary, too long a linker seems also to be a disadvantage as deduced when comparing

Table 1. Melting temperatures of duplexes with monomers **1–6** inserted as a bulge or as an end-positioned intercalating pseudonucleotide.

	5′-AGCTTG–CTTGAG-3′ 3′-TCGAAC**X**GAACTC-5′		5′-GCTTGAG-3′ 3′-CGAACTC**X**-5′	
X	T_m (°C)	ΔT_m (°C)	T_m (°C)	ΔT_m (°C)
–	47.4	–	22.8	–
1	50.4	3.0	33.8	11.0
2	49.4	2.0		
3	47.2	−0.2	31.4	8.6
4	43.8	−3.6	28.4	5.6
5	50.6	3.2	34.4	11.6
6	49.2	1.8		

the duplex stability for insertion **3** with the stability of the duplex from insertion of **1**. The oligo with insertion of the monomer **2**, having a sulphur atom in the linker instead of oxygen, showed almost the same thermal melting temperature as was observed for the insertion of **1**. The stabilization was only 1.0°C in favour of the oxygen analogue. However, whereas the monomer **1** is an (*R*)-enantiomer, the monomer **2** is a racemic mixture. This makes it difficult to draw conclusions for the duplex stabilities for insertion of the individual enantiomers of **2** apart from assuming little dependence on the duplex stability by exchanging oxygen with sulphur in the linker. Finally, the anthraquinone **6** was stabilizing the duplex structure having a melting temperature of 49.2°C corresponding to an increase 1.8°C compared to the wild type duplex.

The dependence on the length of the linker becomes even clearer when intercalating nucleic acid monomers are incorporated as an end-positioning intercalating pseudonucleotide (Table 1). An increase in melting temperature of 5.6°C is seen for **4** compared with the unmodified duplex, whereas **1** and **5** increases the melting temperature with 11.0°C and 11.6°C, respectively. In between is the monomer **3** with an increase of thermal melting of 8.6°C. Here the same trend as above is followed. The intercalating nucleic acid monomers **1** and **5** result in nearly the same affinity for the targets, while **3** with a longer linker is not as efficient as **1**, and **4** having a shorter linker than **5** is contributing with the lowest stabilization to the duplex.

To investigate the dependence on linker length further, some intercalating nucleic acids with two intercalating moieties were prepared. The monomers were inserted with varying distances as neighbours, next-nearest neighbours or with four nucleotides between the monomers. Previously we have focused on the pyrene monomer **1** in the same sequences[2] and its fluorescence properties which confirmed its intercalation rather than groove binding in duplexes.[3] From Table 2 it is seen that it is sufficient for two pyrene insertions to have only one natural base pair between the insertions to improve the duplex stability. For sequences with the monomer **1**, we have previously shown that for this type of double insertions the improved stability was due to intercalation rather than to stacking of the two intercalating agents on its self. This was shown by quenching of a pyrene excimer band on duplex formation.[3] Although one insertion of **3** lowered the duplex melting temperature, two insertions of **3** as next nearest neighbours resulted in an oligo with nearly the same hybridization properties as the wild type oligo. The monomer **5** with increased linker length due to an extra methylene group also in this case with next nearest neighbours increased the melting temperature in a comparable manner to what was observed for the pyrene monomer **1**.

Table 2. Changes in melting temperatures of duplexes with **1**[2], **3**, **4** and **5** inserted as bulges.

X =	**1** ΔT_m (°C)	**3** ΔT_m (°C)	**4** ΔT_m (°C)	**5** ΔT_m (°C)
3′-TCG AAC **XX**G AAC TC-5′	−5.2	−5.0	−14.0	–
3′-TCG AAC **X**G**X** AAC TC-5′	4.0	0.4	−9.6	4.4
3′-TCG A**X**A CGA **X**AC TC-5′	13.4	7.8	−6.2	9.0
3′-TCG AAC **X**G**1** AAC TC-5′			–	5.5

The target sequence was 5′-AGC TTG CTT GAG-3′ and the reference melting temperature for the wild type duplex without insertions was 47.4°C.

Marcel Dekker, Inc.
270 Madison Avenue, New York, New York 10016

Interestingly, the combination of **1** and **5** as next nearest neighbours in the same strand increases the melting of the duplex with 5.5°C, which is nearly the same as, found for same type of double insertion with **1**. The highest stabilizations of the duplexes as determined from increases in melting temperatures were found in case of four natural base pairs between two insertions. In fact the same dependence of duplex stabilities on linker length as for the next-nearest neighbours was found in this case. Again the monomers **1** and **5** show similarity in being the best stabilizers of the duplex in comparison with the monomers **3** and **4**, respectively, which seem to have less appropriate linker lengths. When the monomers **1**, **3** and **4** were double inserted as neighbours a considerable drop in melting temperature was observed. One can imagine that this is due to increased flexibility of the strand with double insertions and difficulties in accommodating the two intercalating ring inside the helix structure.

From molecular calculations (MacroModel) on the DNA/INA™ duplex, we anticipated that the neighbouring nucleobase in the 3′ position of the intercalator (in the same strand) is more crucial for the ability of stacking than the nucleobases of the opposite strand. Therefore the sequence was changed, so the neighbouring bases to the intercalating monomer were either both cytosine or both guanine (Table 3). In both cases the intercalator was placed between two C–G base pairs like in the original sequence from Table 1.

Without intercalators the melting temperature for this new sequence was higher than for the original wild type sequence from Table 1. When the pyrene INA™ **1** was inserted between two cytosines, ΔT_m was marginally higher than for the original sequence (3.3°C compared to 3.0°C). Shifting the intercalator to the complementary strand leads to an increase in melting temperature (ΔT_m = 7.6°C), indicating better stacking when the intercalator is neighbouring two guanines in the same strand. For **3** the ΔT_m was 2.5°C in case of two neighbouring cytosines, which is also an improvement from the corresponding sequence with **3** from Table 1 (ΔT_m = −0.2°C). However, when the intercalator was shifted to the complementary strand, the increase in melting temperature was only 3.6°C compared to the wild type duplex. Thus for this sequence the longer linker in **3** is also a disadvantage when compared with the length of the linker in **1**, showing the necessity for the intercalator to be able to interact with both strands in order to bring about an efficient stabilization effect. We also investigated anthracene **7** as an intercalator in this context. However, anthracene destabilized the duplex and was therefore not interesting for further experiments.

Furthermore we decided to investigate the affinity for triplex formation of intercalating nucleic acids containing the monomers **1** and **3**, as there is a particular

Table 3. Melting temperatures of duplexes **X = 1**, **3** and **7** inserted as a bulge.

Sequences	–(Ref) T_m (°C)	**1** ΔT_m (°C)	**3** ΔT_m (°C)	**7** ΔT_m (°C)
5′-AGCTTG–GTTGAG-3′ 3′-TCGAAC**X**CAACTC-5′	49.6	3.3	2.5	−1.3
5′-AGCTTG**X**GTTGAG-3′ 3′-TCGAAC–CAACTC-5′	49.6	7.6	3.6	–

MARCEL DEKKER, INC.
270 Madison Avenue, New York, New York 10016

interest in the development of DNA intercalators, which can efficiently promote triple helix formation. Usually the stabilization of the triplex structure is observed upon direct addition of the heterocyclic compounds sometimes possessing positively charged side chain to a solution containing all three oligonucleotide sequences.[11,12] Intercalators linked by a polymethylene linker to the 5′-end of the triplex forming oligonucleotide (TFO) have been described.[13–16] Recently we investigated the effects of insertion of 5-methyl-N^4-(1-pyrenylmethyl)-2′-deoxycytidine as a bulge into DNA towards DNA/DNA duplex, three-way junction and triplex structures.[17] In the latter case its insertion as a bulge in the middle of the triplex sequence afforded a 10.4°C increase in the melting temperature compared with the wild type triplex. Therefore it is obvious to suppose a stabilization of the triplex with an intercalating nucleic acid. The intercalating nucleic acid monomers **1** and **3** were inserted as a bulge, as next-nearest neighbours in the middle, and at the 5′-end of the TFO (Table 4). The single insertion in the middle of TFO had no effect on the T_m value in the case of **3** but a drop in T_m of 5°C was observed for **1** compared to the reference TFO system. The insertions of both intercalating nucleic acid monomers as the next-nearest neighbours led to an even more dramatic decrease in melting temperature, which is contrary to the results obtained with duplexes. However, the monomers **1** and **3** linked to the 5′-end of TFO resulted in stabilization of triplexes (ΔT_m of 9.0°C for **1** and 11.0°C for **3**). When the effects of bulge insertions of these monomers into TFO are investigated, it can be concluded that **3** (containing the longer linker) stabilizes the triplex better than does **1**. This is contrary to what is seen for duplexes. Furthermore it could be speculated that further stabilization of the triplexes by the pyrene moiety could be achieved by further increasing the length of the linker to allow more favorable stacking interactions into the duplex strands. This could be observed in the case of 5-methyl-N^4-(1-pyrenylmethyl)-cytidine[17] where the nucleotide was also involved in base stacking and allowed the pyrene moiety being in stronger interactions with neighbouring nucleobases. On the other hand, the considerable stabilization by TFO possessing **1** and **3** at the 5′-end is believed due to the stacking interactions only (the effect as a lid) without disturbing of triple helixes.

To exclude that we were measuring a duplex formation between the T rich TFO and the A rich purine strand, we also determined the melting temperature of the 14-mer TFO hybridized to the 17-mer purine strand. As this mixture had a T_m of 20°C, there was clearly no interference with the triplex measurements in Table 4, except for the examples with next nearest neighbours. However, in this case the conclusion about the dramatically lowering of the triplex melting temperatures is still correct.

Table 4. Melting temperatures of triplex studies with **1** and **3**. The target duplex of 5′-GAC GGG GAA AGA AAA AA-3′ and 3′-CTG CCC CTT TCT TTT TT-5′ showed thermal melting at 58°C.

X =	T_m (°C)	**1** T_m (°C)	**3** T_m (°C)
5′-CCC CTT–TCT TTT TT-3′	36		
5′-CCC CTT**X**TCT TTT TT-3′		31	36
5′-CCC CTT**X**T**X**CT TTT TT-3′		<20	23
5′-**X**CCC CTT TCT TTT TT-3′		45	47

MARCEL DEKKER, INC.
270 Madison Avenue, New York, New York 10016

NMR STUDIES

In order to determine exactly how INA™ intercalate and what consequences the intercalation has for the structure of the duplex, NMR experiments were performed and compared with thermal stability measurements, using **1** as an example. Unfortunately, it turned out that the chosen ATXAT duplex possessed some characteristics that made good quality NMR spectra difficult to obtain and structure determination impossible to perform. The results gained from NMR studies therefore became more vague and quantitative than expected. For the NMR studies we had chosen a 9-mer oligonucleotide, for which NMR data for the DNA:DNA duplex structure was available.[18] **1** was inserted as a bulge in the middle of the duplex in an A–T region. The numbering assignment of the nucleobases in this duplex is shown in Figure 2. Incorporation of INA™ **1** in the strand gives an increase in melting temperature of 10.3°C compared to the unmodified duplex, which melted at 30.9°C.

The first spectra obtained for the ATXAT duplex showed some very broad lines, especially in the aromatic region, therefore a series of dilution experiments were performed to reveal whether this was a concentration dependent characteristic of the sample. From these experiments we realized that there is a dependency of the sample concentration on the line shape of the aromatic protons with lines becoming sharper at low duplex concentration. In order to circumvent this problem another approach was taken, and instead of diluting the sample, DMSO-d_6 was added. This was based on the idea that a change in polarity would decrease the aggregation of the duplex, which was probably the problem at higher concentrations. However, the amount of DMSO added had to be moderate since the addition pushes the stability equilibrium of a DNA duplex towards ssDNA.

The spectra acquired after addition of DMSO displayed cross peaks that could be assigned to the pyrene moiety, but no specific assignment could be performed, suggesting that the pyrene is intercalated as expected but not restrained to one site, thus inducing high mobility and a very flexible core. This theory is supported by the fact that no cross peaks between T13 and A14 can be observed in the spectra, indicating intercalation between these residues or a major disturbance of the normal helical structure. Comparison of the chemical shift changes observed relative to the unmodified duplex[18] support the theory of intercalation. Especially A6:H2 draws attention as this proton is shifted from 7.21 ppm in the unmodified duplex to 6.64 ppm in the ATXAT duplex, a pronounced shift probably due to ring current effects from the intercalating pyrene moiety. Examination of the aromatic protons in the insertion area reveals that A14:H8 and A6:H8 shift downfield 0.44 and 0.26 ppm respectively, whereas no significant shift could be observed for T5:H6 and T13:H6. It is intriguing that the effect of INA™ is more pronounced for the aromatic protons

	1	2	3	4	5		6	7	8	9	
5'-	C	T	G	A	T	**X**	A	T	G	C	-3'
3'-	G	A	C	T	A	—	T	A	C	G	-5'
	18	17	16	15	14		13	12	11	10	

Figure 2. The numbering assignment of the nucleobases in the ATXAT duplex used for NMR studies. The intercalator **1** is denoted **X**.

of A6 and A14 than for T5 and T13, but it is presumably because of the larger ring system of adenine, and thereby the bigger influence from the stacking with the pyrene moiety.

For the changes observed for the sugar protons the picture become more unclear. Here the observed changes are greatest for T5 and T13, whereas A6 and A14 only seem to be under little influence, except for A14:H2′. For the two adenines all the observed shifts are downfield, but for the thymines both upfield and downfield shifts are observed, making predictions of how the pyrene moiety is situated in the duplex difficult.

Exchange peaks for T5 and T7 indicates that the duplex has more than one conformation. This is supported by the fact that neither the aromatic nor the aliphatic pyrene protons can be assigned, indicating that the pyrene moiety may have more than one orientation.

It was peculiar to us that lines in the spectra of the ATXAT were so broad, when insertion of INA™ creates a thermal stabilization of 10.3°C. The answer to this might be the concentration of the duplex. In the measurements of the thermal stability, the concentrations used were approximately 500 times lower (2.5–3.5 μM), than in the NMR experiments (1.36 mM). This suggests that a destabilization might be observed if the concentration had been higher, which is supported by the fact that dilution of the NMR sample gave sharper lines in the spectra.

MOLECULAR MODELING

To learn more about the binding conformations of the intercalating nucleic acid monomers, when incorporated into oligos, conformational searches using Macromodel 8.1[19] were performed. The conformational searches were based on stochastic dynamics simulations followed by multiple minimizations of snapshots collected every 5 picoseconds. In both cases the Macromodel implementation of the Amber force field[20,21] and the GB/SA water model[22] were used.

The most extensive study was performed on a 12-mer duplex having **1** as a bulge. A 2 nanoseconds stochastic dynamics simulation[23] at 300 K yielded 400 structures, which were minimized. The 400 minimized structures showed two main conformations of the pyrene moiety. INA™ monomer **1** and the two neighbouring base pairs for the two main conformations are shown in Figure 3. The calculation shows that the pyrene monomer preferentially stacks to a base pair to the 5′-side and a purine to the 3′-side (upper Figure 3) or to a base pair to the 3′-side and a purine to the 5′-side (lower Figure 3). These findings support the results of the NMR study described above, about a conformational equilibrium.

A smaller study contained four 12-mer duplexes containing intercalating nucleic acid monomers **2–5** as bulges. The duplexes were all subject to a 500 picoseconds stochastic simulation at 300 K leading to 100 structures of each duplex that were minimized. In all four cases only one binding conformation of the intercalating group was observed. Comparison of the binding modes of monomer **2–5** with that of **1** revealed some interesting features. For monomers **1**, **2**, **3** and **5** the aromatic ring system occupied the same space inside the duplex showing that a longer linker like in the case of **3** does not lead to a displacement of the intercalator, but rather a

MARCEL DEKKER, INC.
270 Madison Avenue, New York, New York 10016

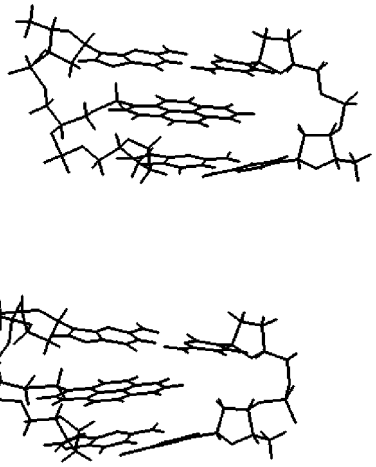

Figure 3. A slice of a calculated structure of the same duplex in two conformations. The top base pair is kept in the same position for the upper and lower figure, showing the pyrene monomer stacking in two different conformations.

change in the backbone to adopt the extra atoms. The calculated binding conformation of monomer **4** shows that the intercalator is not able to reach the same position in the duplex as the four other monomers, leading to a position partially outside the duplex. These results support the findings in the thermal studies where a shortening of the linker (**5** → **4**) was more destabilizing than a lengthening of the linker (**1** → **3**).

CONCLUSION

Through melting temperature studies we have shown dependence on linker length for intercalating nucleic acid monomers exemplified by intercalators pyrene and 7,9-dimethylpyrido[3′,2′:4,5]thieno[3,2-*d*]pyrimidine-4(1*H*)-one. For the latter the difference from one carbon more in the linker increased the affinity to the target strand, while the opposite was the case for pyrene intercalators. In some cases **4** was seen to destabilize the duplex, while **5** was strongly stabilizing the duplex. Hence it is important that the combined length of linker and intercalator is optimal, to obtain a large increase in affinity between the intercalating nucleic acid and the target DNA sequences. Intercalating nucleic acids with the monomers **1** and **5** have nearly the same affinity for their target sequence, even though the intercalating moieties are very different.

The results from molecular calculations and NMR studies support the possibility of a rapid equilibrium between at least two conformations around the site of intercalation of the pyrene monomer **1**. The implication of this equilibrium is that the optimal linker and intercalator combinations have not yet been found and that higher thermal stabilizations are to be reported in the future.

MARCEL DEKKER, INC.
270 Madison Avenue, New York, New York 10016

EXPERIMENTAL

General

NMR spectra were recorded on a Varian Gemini 2000 NMR spectrometer at 300 MHz for ^{1}H and 75 MHz for ^{13}C with TMS as internal standard. EI mass spectra were recorded on a Finnigan Mat SSQ 701 spectrometer, MALDI spectra were recorded on a Fourier Transform Ion Cyclotron Resonance Mass Spectrometer. Elementary analyses were performed at H.C. Ørsted Institute, University of Copenhagen. Silica gel (0.040–0.063 mm) used for column chromatography and analytical silica gel TLC plates 60 F_{254} were purchased from Merck. UV-light or a solution of $(NH_4)_6Mo_7O_{24}\bullet 4H_2O$ (50 g) and $Ce_2(SO_4)_3$ (1 g) in 5% sulphuric acid were used for visualization of TLC. Solvents used for column chromatography were distilled prior to use, while reagents were used as purchased.

General procedure for synthesis of (*S*)-2,2-dimethyl-4-[2-(pyren-1-ylmethoxy)-ethyl]-[1,3]dioxolane (9a) and (S)-4-[2-(anthracen-9-ylmethoxy)-ethyl]-2,2-dimethyl-1,3-dioxolane (9b). To a solution of (S)-(+)-2,2-dimethyl-1,3-dioxolane-4-ethanol (442 mg, 3 mmol or 1.02 g, 7 mmol for reaction with **8a**, **8b**, respectively) in dry toluene (100 mL) was added pulverized KOH (3.82 g, 68 mmol) followed by 1-chloromethylpyrene **8a** (900 mg, 3.6 mmol) or 9-chloromethylanthracene **8b** (1.90 g, 8.4 mmol). A Dean-Starck apparatus was used, while refluxing the reaction mixture for 24 h. H_2O (50 mL) was added and the organic phase was washed with H_2O (3 × 50 mL), dried ($MgSO_4$) and evaporated under reduced pressure giving a brown oil, which was purified by silica gel column chromatography (EtOAc/petroleum ether 25:75, v/v).

9a. Yield: 734 mg (67%) as a yellow oil. ^{1}H NMR ($CDCl_3$): δ 7.96–8.33 (m, 9H, arom), 5.18 (s, 2H, C*H*$_2$), 4.22 (m, 1H, H-2′), 4.01 (m, 1H, H-1′), 3.71 (t, 2H, *J* = 5.4 Hz, H-4′), 3.55 (m, 1H, H-1′), 1.61–1.97 (m, 2H, H-3′), 1.39, 1.33 (2 × s, 6H, 2 × C*H*$_3$). ^{13}C NMR (DMSO-d_6): δ 131.35, 131.25, 131.19, 130.76, 129.26, 127.64, 127.36, 126.84, 125.89, 125.18, 124.43, 123.34 (C-arom), 108.50 (*C*$(CH_3)_2$), 73.82, 71.70, 69.61, 67.13 (C-1′, C-2′, C-4′, CH_2), 33.94 (C-3′), 26.91, 25.73 (C(*C*$H_3)_2$). MS (MALDI): *m*/*z* = 383 (MNa^+).

9b. Yield: 2.12 g (90%) as an oil. ^{1}H NMR ($CDCl_3$): δ 8.43 (s, 1H, arom), 8.35 (d, 2H, *J* = 8.5 Hz, arom), 7.99 (d, 2H, *J* = 7.9 Hz, arom), 7.42–7.55 (m, 4H, arom), 5.44 (s, 2H, CH_2), 3.88–3.93 (m,1H, H-1′), 3.73–3.78 (m, 2H, H-1′ and H-2′), 3.46 (t, 1H, *J* = 7.8 Hz, H-4′), 3.03–3.09 (m, 1H, H-1′), 1.81–1.92 (m, 2H, H-3′), 1.37 (s, 3H, CH_3), 1.32 (s, 3H, CH_3). ^{13}C NMR ($CDCl_3$): δ 131.41, 130.93, 129.30, 128.99, 128.32, 126.12, 124.91, 124.25 (C-arom), 108.46 (*C*$(CH_3)_2$), 73.70, 69.49, 67.17, 65.14 (C-1′, C-2′, C-4′, CH_2), 33.89 (C-3′), 26.89, 25.73 (2 × CH_3).

(*S*)-4-(Pyren-1-ylmethoxy)-butane-1,2-diol (3). Compound **9a** (633 mg, 1.8 mmol) was stirred in 80% acetic acid (100 mL) for 42 h at room temperature. The solvent was evaporated in vacuo to give **3** as a yellow oil in quantitative yield. ^{1}H NMR ($CDCl_3$): δ 7.92–8.28 (m, 9H, arom), 5.15 (s, 2H, CH_2), 4.54 (br s, 2H, 2 × OH), 3.85–3.90 (m, 1H, H-2′), 3.64–3.75 (m, 2H, H-4′), 3.40–3.59 (m, 2H, H-1′), 1.69–1.81 (m, 2H, H-3′). ^{13}C NMR ($CDCl_3$): δ 131.34, 131.13, 130.67, 129.23, 127.84, 127.46, 127.28, 126.96, 125.92,

MARCEL DEKKER, INC.
270 Madison Avenue, New York, New York 10016

125.25, 124.41, 122.98 (C-arom) 71.72, 71.15, 68.08, 66.41 (C-1′, C-2′, C-4′, CH_2), 32.74 (C-3′). MS (MALDI): *m/z* = 343 (MNa^+).

(*S*)-4-(Anthracen-9-ylmethoxy)-butane-1,2-diol (7). Quantitative yield. ^1H NMR (DMSO-d_6): δ 8.63 (s, 1H, arom), 8.43 (d, 2H, J = 8.5 Hz, arom), 8.11 (d, 2H, *J* = 7.9 Hz, arom), 7.51–7.63 (m, 4H, arom), 5.42 (s, 2H, CH_2), 4.51 (br s, 2H, 2 × OH), 3.78 (m, 1H, H-2′), 3.19–3.57 (m, 4H, H-1′, H-4′), 1.48–1.82 (m, 2H, H-3′). ^{13}C NMR (DMSO-d_6): δ 130.85, 130.28, 129.35, 128.69, 127.70, 126.11, 125.04, 124.46 (C-arom), 68.43, 67.19, 65.93, 64.04 (C-1′, C-2′, C-4′, CH_2), 33.72 (C-3′).

(*S*)-1-(4,4′-Dimethoxytriphenylmethyloxy)-4-(pyren-1-ylmethoxy)-butan-2-ol (10a). Compound **3** (515 mg, 1.6 mmol) was dissolved in dry pyridine (10 mL) and dimethoxytrityl chloride (DMT–Cl) (652 mg, 1.9 mmol) was added. The reaction mixture was stirred for 42 h at room temperature. The solvent was evaporated off under reduced pressure, and the residue was purified by silica gel column chromatography (EtOAc/cyclohexane/triethylamine 24:74:2, v/v/v). Yield: 800 mg (80%) as a yellow oil. ^1H NMR ($CDCl_3$): δ 7.95–8.33 (m, 9H, arom), 7.17–7.41 (m, 9H, arom), 6.76 (d, 4H, arom), 5.16 (s, 2H, CH_2), 4.01 (m, 1H, H-2′), 3.70–3.76 (m, 2H, H-4′), 3.72 (s, 6H, 2 × C*H*$_3$O), 3.08–3.11 (m, 2H, H-1′), 2.78 (br s, 1H, OH), 1.82 (m, 2H, H-3′). ^{13}C NMR ($CDCl_3$): δ 158.38, 149.80, 144.88, 136.03, 131.24, 130.76, 129.99, 128.09, 127.73, 127.37, 126.88, 126.68, 125.89, 125.20, 125.18, 124.86, 124.69, 124.46, 123.24, 113.02 (C-arom) 85.91 (C-trityl), 71.68, 69.46, 67.94, 67.23 (C-1′, C-2′, C-4′, CH_2), 55.11 (2 × *C*H_3O), 33.55 (C-3′). HRMS (MALDI): *m/z* calcd for $C_{42}H_{38}O_5Na^+$ (MNa^+): 645.2644, found 645.2621.

(*S*)-4-(Anthracen-9-ylmethoxy)-1-(4,4′-dimethoxytriphenylmethyloxy)-butan-2-ol (10b). Yield: 210 mg (85%) as yellow foam. ^1H NMR ($CDCl_3$): δ 6.77–8.45 (m, 22H, arom), 5.44 (s, 2H, CH_2), 3.82–4.14 (m, 1H, H-2′), 3.79 (s, 6H, 2 × OCH_3), 3.05–3.09 (m, 2H, H-4′), 1.72–2.06 (m, 2H, H-3′). ^{13}C NMR ($CDCl_3$): δ 158.58, 158.38, 147.31, 144.86, 139.44, 136.05, 134.08, 131.38, 130.91, 129.98, 129.10, 128.98, 128.09, 127.74, 127.03, 126.69, 126.20, 124.93, 124.17 (C-arom), 113.13, 113.03 (4 × CH-DMT), 85.89 (C-trityl), 69.41, 68.10, 67.17, 65.20 (C-1′, C-2′, C-4′, CH_2), 55.21, 55.16 (2 × OCH_3), 33.55 (C-3′).

Phosphoramidite of (*S*)-1-(4,4′-dimethoxytriphenylmethyloxy)-4-(pyren-1-ylmethoxy)-butan-2-ol (11a). Compound **10a** (305 mg, 0.5 mmol) was dissolved under N_2 in dry CH_2Cl_2 (7 mL). *N*,*N*-Diisopropylammonium tetrazolide (124 mg, 0.7 mmol) was added followed by dropwise addition of 2-cyanoethyl-*N*,*N*,*N*′,-*N*′-tetraisopropylphosphorodiamidite (302 mg, 1 mmol). The reaction mixture was stirred at room temperature for 24 h. The solvent was evaporated under reduced pressure and the residue was purified by silica gel column chromatography (EtOAc/cyclohexane/triethylamine 49:49:2, v/v/v). Yield: 250 mg (62%) as a colourless oil. ^{31}P ($CDCl_3$): δ 150.25, 149.89. HRMS (MALDI): *m/z* calcd for $C_{51}H_{55}N_2O_6PNa^+$ (MNa^+): 845.3689, found 845.3705.

Phosphoramidite of (*S*)-4-(Anthracen-9-ylmethoxy)-1-(4,4′-dimethoxytriphenylmethyloxy)-butan-2-ol (11b). Yield: 206 mg (83%) as yellow foam. ^1H NMR ($CDCl_3$): δ 6.75–8.45 (m, 22H, arom), 5.43 (2 × s, 2H, CH_2), 4.12 (m, 1H, H-2′), 3.76

MARCEL DEKKER, INC.
270 Madison Avenue, New York, New York 10016

(s, 6H, 2 × OCH_3), 2.53–3.68 (m, 8H, H-1′, H-4′, OCH_2CH_2CN, 2 × $CH(CH_3)$), 2.31 (t, 2H, J = 6.8 Hz, CH_2), 1.89–2.26 (m, 2H, H-3′), 1.10–1.18 (m, 12H, 4 × CH_3). ^{31}P NMR ($CDCl_3$): δ 149.85, 149.55.

3-*N*-(*S*)-2″,2″-Dimethyl-1″,3″-dioxalane-4″-ethanyl)-7,9-dimethylpyrido-[3′,2′:4,5]thieno[3,2-*d*]pyrimidine-4(1*H*)-one (13b). 7,9-Dimethylpyrido-[3′,-2′:4,5]thieno[3,2-*d*]pyrimidine-4(1*H*)-one **12** (1.16 g, 5.0 mmol) was suspended in anhydrous DMF (20 mL) and NaH (0.2 g, 5.0 mmol, 60% dispersion in oil) was added. The mixture was stirred for 2h until all H_2 evolving ceased. Then (*S*)-2,2-dimethyl-1,-3-dioxolane-4-ethanoyl-*O*-*para*-toluenesulfonate (0.78 g, 5.1 mmol) was added and the mixture was stirred for 24h at 80°C. The mixture was evaporated to dryness in vacuo, co-evaporated with dry toluene (3 × 10 mL) in vacuo and the residue was purified by silica gel column chromatography (5% EtOAc in $CHCl_3$) to get a colourless product. Yield: 0.81 g (45%); mp. 119–121°C; IR (KBr): 1676 (CO) cm^{-1}. ^1H NMR ($CDCl_3$): δ 7.22, 7.07 (2 × s, 2H, arom), 4.05–4.36 (m, 4H, 2 × CH_2), 3.61 (m, 1H, CH), 2.91, 2.67 (2 × s, 6H, 2 × CH_3), 1.92–2.20 (m, 2H, CH_2), 1.47, 1.39 (2 × s, 6H, $C(CH_3)_2$). ^{13}C NMR ($CDCl_3$): δ 162.84, 159.87, 157.56, 152.10, 149.56, 146.89, 124.43, 122.59, 122.28 (C-arom), 109.33 ($C(CH_3)_2$), 72.55 (CH), 68.96, 44.51, 32.77 (3 × CH_2), 26.97, 25.51 ($C(CH_3)_2$), 24.51, 19.29 (2 × CH_3). HRMS (MALDI): *m/z* calcd for $C_{18}H_{21}O_3N_3SNa^+$ (MNa^+): 382.1190, found 382.1199. Anal. Calcd for $C_{18}H_{21}O_3N_3S$: C, 60.15; H, 5.89; N, 11.69. Found: C, 60.26; H, 5.90; N, 11.57.

(*S*)-4-(7,9-Dimethylpyrido[3′,2′:4,5]thieno[3,2-*d*]pyrimidine-4(1*H*)-one)-butane-1,2-diol (5). 3-*N*-((*S*)-2″,2″-dimethyl-1″,3″-dioxalane-4″-ethanoyl)-7,9-dimethylpyrido[3′,2′:4,5]thieno[3,2-*d*]pyrimidine-4(1*H*)-one **13b** (0.75 g, 2.1 mmol) was stirred in 80% AcOH (20 mL) for 24h at room temperature. The product was obtained by concentration in vacuo and co-evaporation with EtOH. The residue was purified by silica gel column chromatography (5% MeOH in $CHCl_3$) to get the colourless product. Yield: 0.50 g (75%); mp. 104–106°C. ^1H NMR (DMSO): δ 8.58, 7.28 (2 × s, 2H, arom), 4.52–4.76 (m, 2H, 2 × OH), 4.08–4.25 (m, 2H, CH_2), 3.26–3.49 (m, 3H, CH_2 and CH), 2.87, 2.59 (2 × s, 6H, 2 × CH_3), 1.69–1.95 (m, 2H, CH_2). ^{13}C NMR (DMSO): δ 160.96, 159.16, 156.26, 151.16, 149.25, 145.90, 123.42, 122.19, 120.03 (C-arom), 68.19 (CH), 65.29, 43.50, 32.02 (3 × CH_2), 23.29, 18.27 (2 × CH_3). MS–EI: *m/z* = 319 (M^+, 10), 301 (20), 232 (100). Anal. Calcd for $C_{15}H_{17}N_3O_3S$: C, 56.41; H, 5.37; N, 13.16. Found: C, 55.84; H, 5.38; N, 12.77.

(*S*)-1-(4,4′-Dimethoxytriphenylmethyloxy)-4-(7,9-dimethylpyrido[3′,2′:4,5] thieno[3,2-*d*]pyrimidine-4(1*H*)-one)-2-butanol (14b). (*S*)-4-(7,9-Dimethylpyrido[3′,2′:4,5]thieno[3,2-*d*]pyrimidine-4(1*H*)-one)-butan-1,2-diol **5** (0.6 g, 1.9 mmol) was dissolved in dry pyridine (5 mL) and DMT–Cl (0.71 g, 2.1 mmol) was added. The reaction mixture was stirred at room temperature overnight. It was concentrated in vacuo and co-evaporated with dry toluene (3 × 10 mL). The residue was purified by silica gel column chromatography (EtOAc/cyclohexane/triethylamine 49:49:2, v/v/v) to yield a white foam. Yield: 0.77 g (65%); mp. 134–136°C. ^1H NMR ($CDCl_3$): δ 8.22 (s, 1H, arom), 6.78–7.40 (m, 14H, arom), 4.21–4.24 (m, 2H, CH_2), 3.75 (s, 6H, 2 × OCH_3), 3.61–3.69 (m, 2H, CH and OH), 3.11–3.14 (m, 2H, CH_2), 2.93, 2.67, (2 × s, 6H, 2 × CH_3), 1.79–2.45 (m, 2H, CH_2). ^{13}C NMR ($CDCl_3$): δ 162.93, 159.94, 158.48, 157.93, 152.25, 147.77, 146.97, 144.57, 135.74, 135.33, 129.92, 128.02,

Marcel Dekker, Inc.
270 Madison Avenue, New York, New York 10016

127.83, 126.84, 124.52, 122.66, 113.13 (C-arom), 86.26 (C-trityl), 67.22 (CH), 55.15 ($2 \times OCH_3$), 66.72, 43.92, 32.37 ($3 \times CH_2$), 24.55, 19.33 ($2 \times CH_3$). HRMS (MALDI) *m/z* calcd for $C_{36}H_{35}N_3O_5SNa^+$ (MNa^+): 644.2190, found 644.2190.

(*S*)-1-(4,4′-Dimethoxytriphenylmethyloxy)-3-(7,9-dimethylpyrido[3′,2′:4,5]-thieno[3,2-*d*]pyrimidine-4(1*H*)-one)-2-propanol (14a). Yield: 0.78 g (65%); mp. 80–83°C. ^{1}H NMR ($CDCl_3$): δ 8.13 (s, 1H, arom), 6.80–7.45 (m, 14H, arom), 4.31–4.42 (m, 1H, CH), 4.25 (br s, 1H, OH), 3.75 (s, 6H, $2 \times OCH_3$), 3.46–3.49 (m, 2H, CH_2), 3.23–3.25 (m, 2H, CH_2), 2.87, 2.66 ($2 \times$ s, 6H, $2 \times CH_3$). ^{13}C NMR ($CDCl_3$): δ 162.94, 160.02, 158.64, 158.50, 152.36, 148.35, 147.15, 144.58, 135.67, 129.35, 128.23, 128.08, 126.99, 124.50, 122.72, 121.91, 113.31 (C-arom), 86.56 (C-trityl), 69.15 (CH), 55.26 ($2 \times OCH_3$), 64.66, 50.61 ($2 \times CH_2$), 24.61, 19.41 ($2 \times CH_3$). MS–EI: *m/z* = 304 (M^+-DMT, 30); 303 (DMT^+, 100). Anal. Calcd for $C_{35}H_{33}N_3O_5S$: C, 69.17; H, 5.47; N, 6.91. Found: C, 68.44; H, 5.41; N, 6.73.

Phosphoramidite of (*S*)-1-(4,4′-dimethoxytriphenylmethyloxy)-4-(7,9-dimethylpyrido[3′,2′:4,5]thieno[3,2-*d*]pyrimidine-4(1*H*)-one)-2-butanol (15b). (*S*)-1-(4,-4′-Dimethoxytriphenylmethyloxy)-4-(7,9-dimethylpyrido[3′,2′:4,5]thieno[3,2-*d*]pyrimidine-4(1*H*)-one)-2-butanol **14b** (310 mg, 0.5 mmol) was dissolved under N_2 in anhydrous CH_2Cl_2 (10 mL). *N*,*N*-Diisopropylammonium tetrazolide (0.11 g, 0.67 mmol) was added followed by dropwise addition of 2-cyanoethyl-*N*,*N*,*N*′,*N*′-tetraisopropylphophorodiamidite (0.3 g, 1.0 mmol). The reaction was stirred overnight under N_2, concentrated in vacuo and purified by silica gel column chromatography (EtOAc/cyclohexane/triethylamine 49:45:12, v/v/v) to give a white foam. Yield: 345 mg (84%). ^{1}H NMR ($CDCl_3$): δ 8.14 (s, 1H, arom), 7.16–7.39 (m, 10H, arom), 6.73–6.80 (m, 4H, arom), 4.43–4.55 (m, 1H, CH), 3.57 (s, 6H, $2 \times OCH_3$), 3.18–3.56 (m, 10H, $4 \times CH_2$, $2 \times$ NCH), 2.66, 2.79 ($2 \times$ s, 6H, $2 \times CH_3$), 2.42–2.47 (m, 2H, CH_2CN), 0.86–1.34 (m, 12H, $4 \times CH_3$). ^{31}P NMR ($CDCl_3$): δ 149.78, 149.39.

Phosphoramidite of (*S*)-1-(4,4′-dimethoxytriphenylmethyloxy)-3-(7,9-dimethylpyrido[3′,2′:4,5]thieno[3,2-*d*]pyrimidine-4(1*H*)-one)-2-propanol (15a). Yield: 323 mg (80%). ^{1}H NMR ($CDCl_3$): δ 8.12 (s, 1H, arom), 7.16–7.39 (m, 10H, arom), 6.77–6.80 (m, 4H, arom), 4.52–4.57 (m, 1H, OCH), 4.32–4.43 (m, 2H, OCH_2), 3.98–4.02 (m, 2H, $2 \times$ NCH), 3.77 (s, 6H, $2 \times OCH_3$), 3.50–3.54 (m, 2H, CH_2), 3.15–3.33 (m, 2H, CH_2), 2.89, 2.67 ($2 \times$ s, 6H, $2 \times CH_3$), 2.42–2.49 (m, 2H, CH_2CN), 0.84–1.33 (m, 12H, $4 \times CH_3$). ^{31}P NMR ($CDCl_3$): δ 150.73, 150.45.

3-(Pyren-2-ylmethylthio)-propane-1,2-diol (2). 1-Chlormethylpyrene **8a** (269 mg, 1 mmol), 3-mercapto-1,2-propanediol (108 mg, 1 mmol) and triethylamine (200 mg, 2 mmol) were dissolved in dry toluene (20 mL) under N_2. The reaction mixture was stirred at room temperature for 20 h. The pale yellow powder was filtered off and recrystallized from EtOAc. Yield: 90% as yellow crystals; m.p. 90°C. ^{1}H NMR (DMSO-d_6): δ 8.09–8.55 (m, 9H, arom), 4.94 (s, 2H, CH_2), 4.65 (m, 1H, H-2′), 3.48 (m, 2H, H-1′), 2.59 (m, 2H, H-3′).

2-(2,3-Dihydroxy-propylthiomethyl)-anthraquinone (6). 3-Mercapto-1,2-propanediol (108 mg, 1 mmol), 2-bromomethylanthraquinone **16b** (301 mg, 1 mmol) and triethylamine (200 mg, 2 mmol) were dissolved in dry DMF (10 mL) and stirred at

room temperature for 16 h. The solvent was evaporated off under reduced pressure. The pale yellow powder was recrystallized from EtOAc. Yield: 78% as yellow powder; m.p. 110°C. ^{1}H NMR (DMSO-d_6): δ 7.84–8.15 (m, 7H, arom), 3.99 (m, 2H, CH_2), 3.66 (m, 1H, H-2′), 3.39 (m, 2H, H-3′), 2.55 (m, 2H, H-1′).

1-(4,4′-Dimethoxytriphenylmethyloxy)-3-(pyren-2-ylmethylthio)-propan-2-ol (17a). Compound **2** (100 mg, 0.31 mmol) and dimethoxytrityl chloride (140 mg, 0.36 mmol) were dissolved in dry pyridine (5 mL). The reaction mixture was stirred 24 h at room temperature. The solvent was evaporated off under reduced pressure and the residue was purified by silica gel column chromatography (EtOAc/cyclohexane/triethylamine 49:49:2, v/v/v). Yield: 66% as a yellow oil. ^{1}H NMR (DMSO-d_6): δ 6.76–8.35 (m, 22 H, arom), 4.40 (s, 2H, CH_2), 3.78 (m, 1H, H-2′), 3.74 (s, 6H, 2 × OCH_3), 3.20 (m, 2H, H-1′) 2.87 (m, 2H, H-3′). ^{13}C NMR (DMSO-d_6): δ 158.46, 144.70, 135.82, 130.67, 130.00, 129.37, 129.11, 128.06, 127.82, 127.39, 126.80, 126.02, 125.27, 129.54, 123.26 (C-arom), 86.20 (C-trityl), 69.73 (C-2′), 66.31, 66.17 (C-1′, C-3′), 55.18 (CH_2), 36.00, 34.54 (2 × CH_3O).

2-[3-(4,4′-Dimethoxytriphenylmethyloxy)-2-hydroxy-propylthiomethyl]-anthraquinone (17b). Compound **16b** (170 mg, 0.5 mmol) and dimethoxytrityl chloride (213 mg, 0.55 mmol) were dissolved in dry pyridine (10 mL). The reaction mixture was stirred at room temperature for 16 h. The solvent was evaporated off under reduced pressure, and the residue was purified by silica gel column chromalography (EtOAc/cyclohexane/triethylamine 49:49:2, v/v/v). Yield: 74% as a colourless oil. ^{1}H-NMR (DMSO-d_6): δ 6.97–8.29 (m, 17H, arom) 3.82 (m, 2H, CH_2), 3.78 (s, 6H, 2 × CH_3O), 3.26 (m, 1H, H-2′), 2.63 (m, 2H, H-1′). ^{13}C NMR (DMSO-d_6): δ 182.83, 188.64 (2 × C═O), 158.43, 145.41, 144.57, 135.72, 134.48, 134.06, 133.99, 133.41, 129.39, 128.96, 128.15, 128.01, 127.79, 127.64, 127.41, 127.14, 126.81, 113.09 (C-arom), 86.26 (C-trityl), 72.12 (C-2′), 69.86, 66.02 (C-1′, C-3′), 55.12 (CH_2), 36.29, 35.26 (2 × CH_3O).

Phosphoramidite of 1-(4,4′-dimethoxytriphenylmethyloxy)-3-(pyren-2-ylmethylthio)-propan-2-ol (18a). Compound **17a** (100 mg, 0.33 mmol) and *N*,*N*-diisopropylammonium tetrazolide (180 mg, 0.50 mmol) were dissolved in 10 mL dry CH_2Cl_2 under N_2. 2-Cyanoethyl-*N*,*N*-diisopropylchlorophosphoramidite (133 mg, 0.6 mmol) was added dropwise. The reaction mixture was stirred 48 h at room temperature. The reaction mixture was quenched by addition of methanol (0.5 mL) and washed with sat. $NaHCO_3$ (3 × 15 mL). The organic layer was dried over Na_2SO_4 and evaporated in vacuo. The product was purified by silica gel column chromatography (cyclohexane/EtOAc/triethylamine 69:29:2, v/v/v). Yield: 62% as a colourless oil. ^{13}P NMR ($CDCl_3$): δ 150.33, 149.94.

Phosphoramidite of 2-[3-(4,4′-dimethoxytriphenylmethyloxy)-2-hydroxy-propylthiomethyl]-anthraquinone (18b). Compound **17b** (165 mg, 0.25 mmol), 2-cyanoethyl-*N*,*N*-diisopropylchlorophosphoramidite (111 mg, 0.50 mmol) and *N*,*N*-diisopropylammonium tetrazolide were dissolved in dry CH_2Cl_2 (10 mL). The reaction mixture was stirred at room temperature for 48 h. The reaction mixture was quenched by adding methanol (0.5 mL) and H_2O (150 mL). The organic layer was separated,

MARCEL DEKKER, INC.
270 Madison Avenue, New York, New York 10016

dried (Na_2SO_4) and the solvent was evaporated in vacuo. The product was purified by silica gel column chromatography (cyclohexane/EtOAc/triethylamine 69:29:2, v/v/v). Yield: 86% as a colourless oil. ^{13}P NMR ($CDCl_3$): δ 150.10, 149.75.

NMR Experiments

The NMR experiments were performed on a Varian INOVA 600 spectrometer at 25°C. NOESY spectra in D_2O were acquired using 2048 complex points in t_2 and a spectral width of 6000 Hz. A total of 512 t_1 experiments were recorded using the States phase cycling scheme. The residual signal of HOD was removed by low-power presaturation. NOESY spectra in H_2O at 5°C and 25°C were obtained using the watergate pulse sequence. The spectra were acquired with 2048 complex points in t_2 and a spectral width of 12000 Hz. A total of 512 t_1 experiments were recorded using the States phase cycling. TOCSY spectra with mixing times of 30 and 70 ms and DQF–COSY spectra were obtained using the States phase cycling scheme. Dilution and DMSO titration 1D experiments were performed on a Varian Unity 500 spectrometer at 25°C with a spectral width of 5000 Hz. All the acquired data were processed using FELIX (Version 98, MSI, San Diego, CA). All spectra were apodized by a skewed sine bell squared in F1 and F2.

Oligonucleotide Synthesis, Purification and Melting Temperature Determination

The ODN syntheses were carried out on an Expedite™ Nucleic Acid Synthesis System Model 8909 from Applied Biosystems. The appropriate amidite was dissolved in a 1:1 mixture of dry MeCN and CH_2Cl_2, as a 0.1 M solution, and inserted into the growing oligonucleotides chain using the same conditions as for normal nucleotide couplings (2 min coupling time). The ODNs were synthesized with DMT on and purified on a Waters Prep LC 4000 HPLC with a Waters Prep LC controller and a Waters 2487 Dual λ Absorbance detector on a Waters Xterra™ MS C_{18} column. Buffer A [950 ml of 0.1 M NH_4HCO_3 and 50 ml of MeCN, (pH = 9.0)] and buffer B [250 ml of 0.1 NH_4HCO_3 and 750 ml of MeCN, (pH = 9.0)] Gradients: 5 min. 100% A, linear gradient to 70% B in 30 min., 2 min. with 70% B, linear gradient to 100% B in 8 min. and then 100% A in 15 min (product peak at ~ 37 min). The ODNs were DMT deprotected in 100 μL 80% acetic acid and precipitated from ethanol.

All modified ODNs were confirmed by MALDI–TOF analysis on a Voyager Elite Bio spectrometry Research Station from Perceptive Biosystems. Melting temperature measurements were performed on a Perkin–Elmer UV/VIS spectrometer fitted with a PTP-6 temperature programmer. Melting temperature (T_m) measurements for duplex studies were determined a 1 mM EDTA, 10 mM $Na_2HPO_4 \cdot 2H_2O$, 140 mM NaCl buffer at pH = 7.0 for 1.5 μM of each strand. Melting temperature measurements for triplex studies were determined in a 10 mM NaOAc, 0.5 M NaCl buffer at pH = 5.5. The triplexes were formed by first mixing the two strands of the Watson-Crick duplex, each at a concentration of 1.0 μM. The solution was heated to 80°C, cooled to room temperature where the third (TFO) strand was added and then kept at 15°C for 30 min. The melting temperature was determined as the maximum of the first derivative

MARCEL DEKKER, INC.
270 Madison Avenue, New York, New York 10016

plots of the melting curve and is with an uncertainty ± 1.0°C as determined by repetitive experiments.

REFERENCES

1. Louët, S. Human genetic signatures. Nat. Biotechnol. 23 June **2003** http://dx.doi.org/10.1038/bioent748.
2. Christensen, U.B.; Pedersen, E.B. Intercalating nucleic acids containing insertions of 1-*O*-(1-pyrenylmethyl)glycerol: stabilisation of dsDNA and discrimination of DNA over RNA. Nucleic Acids Res. **2002**, *30*, 4918–4925.
3. Christensen, U.B.; Pedersen, E.B. Intercalating nucleic acids with pyrene nucleotide analogues as next-nearest neighbours for excimer fluorescence detection of single point mutations under nonstringent hybridisation conditions. Helv. Chim. Acta **2003**, *86*, 2090–2097.
4. Ossipov, D.; Zamaratski, E.; Chattopadhyaya, J. Dipyrido[3,2-*a*:2′,3′-*c*]phenazine-tethered oligo-DNA: synthesis and thermal stability of their DNA•DNA and DNA•RNA duplexes and DNA•DNA•DNA triplexes. Helv. Chim. Acta **1999**, *82*, 2186–2200.
5. Lerman, L.S. Structural considerations in the interaction of deoxyribonucleic acid and acridines. J. Mol. Biol. **1961**, *3*, 18–20.
6. Mori, K.; Ikunaka, M. Synthesis of all of the four energetically possible stereoisomers of 7-ethyl-2-methyl-1,6-dioxaspiro[4.5]decane: a pheromone produced by bees *Paravespura vulgaris l.* and *Andrena haemorrhoa F*. Tetrahedron **1984**, *40*, 3471–3479.
7. Hayashi, H.; Nakanishi, K.; Brandon, C.; Marmur, J. Structure and synthesis of dihydroxypentyluracil from bacteriophage SP-15 deoxyribonucleic acid. J. Am. Chem. Soc. **1973**, *95*, 8749–8757.
8. Schmidt, U.; Kubitzek, H. Thiopyridone aus cyan-thioacetamid. Chem. Ber. **1960**, *93*, 1559–1565.
9. Hassan, K.M.; Kamal El-Dean, A.M.; Youssef, F.; Atta, M.; Abbady, M.S. Synthesis and reactions of some thienopyridine derivatives. Phosporous, Sulfur, Silicon Relat. Elem. **1990**, *47*, 181–189.
10. Gewald, K.; Jänsch, H.J. 3-Amino-furo[2.3-b]pyridine. J. Prakt. Chem. **1976**, *318*, 313–320.
11. Marchand, C.; Bailly, C.; Nguyen, C.H.; Bisagni, E.; Garestier, T.; Hélène, C.; Waring, M.J. Stabilization of triple helical DNA by a benzopyridoquinoxaline intercalator. Biochemistry **1996**, *35*, 5022–5032.
12. Kukreti, S.; Sun, J.-S.; Loakes, D.; Brown, D.M.; Nguyen, C.-H.; Bisagni, E.; Garestier, T.; Helene, C. Triple helices formed at oligopyrimidine•oligopurine sequences with base pair inversions: effect of a triplex-specific ligand on stability and selectivity. Nucleic Acid Res. **1998**, *26*, 2179–2183.
13. Puri, N.; Zamaratski, E.; Sund, C.; Chattopadhyaya, J. Synthesis of 5′-polyarene-tethered oligo-DNAs and the thermal stability and spectroscopic properties of their duplexes and triplexes. Tetrahedron **1997**, *53*, 10409–10432.
14. Mouscadet, J.-F.; Ketterle, C.; Goulaouic, H.; Carteau, S.; Subra, F.; Le Bret, M.; Auclair, C. Triple helix formation with short oligonucleotide-intercalator

conjugates matching the HIV-1 U3 LTR end sequence. Biochemistry **1994**, *33*, 4187–4196.
15. Giovannangéli, C.; Thuong, N.T.; Hélène, C. Oligodeoxynucleotide-directed photo-induced cross-linking of HIV proviral DNA via triple-helix formation. Nucleic Acid Res. **1992**, *20*, 4275–4281.
16. Mohammadi, S.; Slama-Schwok, A.; Leger, G.; El Manouni, D.; Shchyolkina, A.; Leroux, Y.; Taillandier, E. Triple helix formation and homologous strand exchange in pyrene-labeled oligonucleotides. Biochemistry **1997**, *36*, 14836–14844.
17. Abdel-Rahman, A.A.-H.; Ali, O.M.; Pedersen, E.B. Insertion of 5-methyl-N^4-(1-pyrenylmethyl)cytidine into DNA. duplex, three-way junction and triplex stabilities. Tetrahedron **1996**, *52*, 15311–15324.
18. Jensen, G.A.; Singh, S.K.; Kumar, R.; Wengel, J.; Jacobsen, J.P. A comparison of the solution structures of an LNA:DNA duplex and the unmodified DNA:DNA duplex. J. Chem. Soc., Perkin Trans. 2 **2001**, 1224–1232.
19. Mohamadi, F.; Richards, N.G.J.; Guida, W.C.; Liskamp, R.; Lipton, M.; Caufield, C.; Chang, G.; Hendrickson, T.; Still, W.C. MacroModel—an integrated software system for modeling organic and bioorganic molecules using molecular mechanics. J. Comp. Chem. **1990**, *11*, 440–467. See http://www.schrodinger.com.
20. Weiner, S.J.; Kollman, P.A.; Case, D.A.; Singh, U.C.; Ghio, C.; Alagona, G.; Profeta, S., Jr.; Weiner, P. A new force field for molecular mechanical simulation of nucleic acids and proteins. J. Am. Chem. Soc. **1984**, *106*, 765–784.
21. Weiner, S.J.; Kollman, P.A.; Nguyen, D.T.; Case, D.A. An all atom force field for simulations of proteins and nucleic acids. J. Comp. Chem. **1986**, *7*, 230–252.
22. Qiu, D.; Shenkin, P.S.; Hollinger, F.P.; Still, W.C. The GB/SA continuum model for solvation. A fast analytical method for the calculation of approximate born radii. J. Phys. Chem., A **1997**, *101*, 3005–3014.
23. van Gunsteren, W.F.; Berendsen, H.J.C. A leap-frog algorithm for stochastic dynamics. Mol. Simul. **1988**, *1*, 173–185.

Received August 26, 2003
Accepted October 6, 2003

Request Permission or Order Reprints Instantly!